Thermodynamic and experimental study of 30 wt-%Cr-containing Co, Fe or Ni-based alloys with very high contents in Ta and C

Patrice Berthod, Laura Corona

Thermodynamic and experimental study of 30wt.%Cr-containing {Co,Fe or Ni}-based alloys with very high contents in Ta and C

Patrice Berthod* and Laura Corona

Institut Jean Lamour (UMR CNRS 7198)
Department Chemistry and Physics of Solids and Surfaces
Team “Surface and Interfaces, chemical reactivity of materials”
Faculty of Sciences and Technologies, Boulevard des Aiguillettes, B.P. 70239, 54506 Vandoeuvre-lès-Nancy, France

*Corresponding author:

Phone: (+33)383684666, Fax; (+33)383684611,

E-mail: patrice.berthod@univ-lorraine.fr

Postprint version of the article:
Canadian Metallurgical Quarterly 2017 VOL 56 N° 1, 113-122.
DOI: 10.1080/00084433.2016.1267298

Abstract:

TaC carbides are among the most efficient particles for reinforcing cast refractory alloys and superalloys against mechanical stresses at temperature as high as 1000°C and over. The most common TaC-strengthened superalloys contain less than 0.5 wt.%C and 5wt.%Ta. Enriching alloys in C and Ta may lead to higher fractions in TaC and therefore possibly to higher mechanical properties for service in hot conditions. The present work explores the microstructures achievable in a cobalt alloy, a nickel one and an iron one, by the introduction of 1 wt.%C and 15wt.%Ta, first using thermodynamic calculations and second by real elaboration. High fractions in TaC were effectively obtained, script-like eutectic ones, but also blocky pre-eutectic ones less efficient for reinforcement. These blocky TaC, the formation of which was explained by thermodynamic calculations, tend to aggregate together in some locations, with an overconsumption of Ta. However, some disagreements were noticed between predictions with thermodynamic calculations and as-cast microstructures.

Keywords: Cobalt alloy; Nickel alloy; Iron alloy; Tantalum carbides; Solidification; Thermodynamic calculations; As-cast microstructures

Introduction:

Among the different carbides able to efficiently reinforce alloys, the tantalum carbides (TaC) are well-recognized, especially for uses at elevated temperatures. This carbide can be first met in coatings for strengthening the surfaces of some pieces[1], notably for improving the tribology properties[2-4]. It can be present also in bulk materials, e.g. as carbides' alloys[5-7]. Tantalum carbides are also used to strengthen copper-based alloys[8], alloyed steels[9,10], titanium-based[11] and molybdenum-based[12] alloys. Besides coating techniques and sintering route, TaC carbides can precipitate during solidification, and are in equiaxed alloys and even in directionally solidified alloys[13]. Numerous iron-based alloys rich in Al[14,15], or chromium[16,17], Cr-rich nickel-based[18-21] and cobalt-based alloys[22,23] (notably including the well-known Mar-M Co-based superalloy[24], for example), are also strengthened by TaC. Thanks to its stability at high temperature, much higher than the chromium carbides, tantalum carbides are considered as very efficient particles for creep-resistance for long times.

The corrosion-resistant cast superalloys reinforced by TaC carbides effectively represent an important family of high temperature alloys able to simultaneously resist corrosion by aggressive molten substances, oxidation by mixed oxidant gases and mechanical stresses at elevated temperatures. Generally their carbon contents are close to 0.1-0.5 wt.%C, and the most often, lower than 1 wt.%. Their tantalum contents, a rather expensive metal, are also not very high, with values never higher than 10 wt.%.

One can think that the simultaneous presence of more carbon and more tantalum than usual may potentially lead to very high fractions of tantalum carbides, and consequently to especially high mechanical properties. Data about the metallurgical state of such alloys are obviously not available in the literature. It is thus very interesting to explore the microstructures of cobalt-based, nickel-based and iron-based alloys very rich in C and Ta, to discover how carbides can be present in terms of quantity and morphology. This is what was done in the current work, with cast {Co, Ni or Fe-30Cr}-based alloys with 1 wt.% C and 15 wt.%Ta as targeted contents for carbon and tantalum.

Experimental details of the study

Choice of the alloys

Three alloys were considered in this study (all contents being in weight percent): a Co(bal.)-30Cr-1C-15Ta alloy (thereafter named “COhighTaC”), a Ni(bal.)-30Cr-1C-15Ta alloy (“NIhighTaC”), and a Fe(bal.)-30Cr-1C-15Ta alloy (“FEhighTaC”).

Cobalt, nickel and iron were chosen as base elements. They are the most encountered base elements in refractory metallic alloys manufactured by casting, rich in chromium for high temperature chemical resistance, and strengthened by carbides for high temperature mechanical resistance. To avoid too high cost of the alloys, as well as possible metallurgical instabilities, the tantalum content was limited to 15 wt.%. To favor carbides of only a single type, TaC, the carbon content was rated to 1 wt.% (these two weight contents correspond to the molar equivalence between the two elements).

Preliminary thermodynamic calculations

Before manufacturing the three alloys, thermodynamic calculations were carried out using the Thermo-Calc version N software[25]. It worked with the SSOL database[26] enriched with the descriptions of binary and ternary systems involving tantalum (Ta-C[27], Co-Ta[28], Ta-Cr[29] and Co-Ta-C[30]). For each alloy, the calculations started by the determination of the theoretical liquidus and solidus temperatures, which were compared to the experimentally determined ones. Knowing the solidification range is important for processing melting and casting, and also for anticipating the risks of shrinkage defects, as well as the refractoriness of the alloys (important for their high temperature service capability).

Thereafter, successive equilibria were computed to ascertain the metallurgical state of the alloys for different temperatures during cooling, until the end of the theoretical solidification. First, this allowed verifying whether the TaC phase would be the only carbide present, or if other carbides may appear. Since chromium is carbide-former, chromium carbides may also appear, especially as its content was chosen high enough to allow the alloys to resist high temperature oxidation and hot corrosion. Second, knowing the evolution of the chemical compositions of the phases theoretically existing at the successive temperatures, may be important for

interpreting the observed microstructures. Knowing how the chemical composition of the liquid phase varies during cooling is particularly important for anticipating possible segregation.

Casting of the experimental alloys

The three alloys were synthesized by high frequency induction melting of pure cobalt (or nickel or iron), chromium, tantalum (>99.9%, Alfa Aesar) and carbon (pure graphite) together, in a CELES high frequency induction (300 kHz) furnace. An inert atmosphere of 300mbars of argon was created in the fusion chamber to avoid oxidation of the different metals and of carbon. Fusion and solidification were achieved in the water-cooled copper crucible of the furnace. After the heating, the obtained molten alloy was maintained three minutes to achieve the total chemical homogenization of the liquid. This one, with a round shape, was levitating without any contact with the crucible. During the first part of cooling (induced by slow decreasing in injected power) the solidifying molten alloy was still in levitation (separated from the crucible by several millimeters of argon) and when the power was low enough it entered in contact with the copper crucible. At this time faster cooling start, in the solid state for the alloy now almost totally solid. If it can be reasonably thought that the solidification progress was realized according the almost thermodynamic equilibrium conditions, the solid state cooling did not respect these conditions, probably.

The obtained ingots (which were all of about 40g) were cut for obtaining, per alloy, a part destined to study the obtained microstructure and its chemical composition. In parallel, a smaller part (approximate dimensions 2 × 2 × 7mm^3) was also cut, for differential thermal analysis (DTA) using a TG/ATD 92-16.18 SETARAM equipment.

Preparation and metallographic characterization

The as-cast microstructures of the alloys were observed after preparation of metallographic samples. This was done by embedding the cut parts in molds which were filled by a cold resin mixture (Escil resin CY230 + hardener HY956). They were first ground using SiC paper from 120 to 1200 grid under water, and second, after ultrasonic cleaning, polished using a textile enriched with 1µm hard particles.

The different phases present in the as-cast alloys were identified by X-Ray Diffraction (XRD) experiments, performed using a Philips X'Pert Pro diffractometer (Cu Kα, 1.5406Å). A Scanning Electron Microscope (SEM) (JEOL JSM 6010 LA) was used for the metallographic characterization, imaging in the back scattered electron (BSE) mode and global or spot chemical analysis using the energy dispersion spectrometer (EDS) on the SEM, under an acceleration voltage of 20kV.

Results

Preliminary thermodynamic calculations for the COhighTaC alloy

First calculations were carried out with Thermo-Calc, first to compute the three {wt.%Cr; T}-sections for {1wt.%C; 15 wt.%Ta} of the M-Cr-C-Ta systems. Fig. 1 shows that the COhighTaC alloy should start its solidification by the crystallization of the TaC phase. This progresses during a 150°C-cooling, before the start of development of the FCC cobalt-based matrix. This one develops alone over a narrow temperature range, before precipitating together with additional TaC carbides to form a {matrix + TaC} eutectic compound. After 150°C of cooling again, a third solid phase should appear in the previous double-phased alloy: the $Cr_{23}C_6$ carbide phase. The solid-state growth of this second carbide goes on over about 100°C, before the precipitation of a fourth phase: the TCP phase σ (Co-Cr). Below, the σ phase disappears, while the FCC matrix transforms into the low temperature specie of Co-based solid solution: the HCP phase.

More quantitative data are presented in Fig. 2. The curves, plotted in this graph from calculations carried out every 50 or 100°C, show the evolution with temperature of the mass fractions of the successive phases during their appearance or disappearance. Seemingly, about 5 mass.% of TaC develops before the appearance of the matrix, which grows forming an {matrix + TaC} eutectic compound with TaC. At the end of solidification, there is theoretically about 15 mass.% of TaC phase. This does not significantly evolve before 1200°C, temperature for which the calculated mass fractions of TaC is given in Table 1 together with its corresponding volume fraction. One can see also that the fraction of chromium carbides, which appears above 1150°C and remains at least down to 800°C, are very low. The sigma

phase, which is supposed to appear and disappear just after, temporarily exists but with extremely low fraction (not plotted).

Preliminary thermodynamic calculations for the NIhighTaC alloy

The vertical section describing the metallurgical states of the NIhighTaC alloy in the {wt.Cr, T} section for 1wt.%C and 15wt.%Ta is displayed in Fig. 3. Solidification should start here too with the crystallization of a carbide phase. This one is not the TaC carbide but the “high temperature” chromium carbide Cr_7C_3. The matrix starts appearing only after about 100°C of cooling, before the last part of solidification leading to a {matrix + Cr_7C_3} eutectic compound around 1250°C. After total solidification solid state transformations occurred for Cr_7C_3 which is replaced by $Cr_{23}C_6$, and with the precipitation of a Ta-rich phase which is not TaC but a Ni_3Ta intermetallic compound.

For this second alloy, the evolutions of the mass fractions of the different phases are also plotted versus temperature in Fig. 4. The Cr_7C_3 carbides should precipitate over a 150°C-cooling as a single pre-eutectic phase until reaching about 5 mass.%. Thereafter, additional Cr_7C_3 would appear together with the FCC matrix. The total Cr_7C_3 mass fraction reaches about 10 mass.% at the end of solidification, near which a great fraction of them transforms into $Cr_{23}C_6$. At the same time, the Ni_3Ta phase appears. At 1200°C, the alloy is thus composed of two types of chromium carbides and the Ta-rich intermetallic compound (Table 1).

Preliminary thermodynamic calculations for the FEhighTaC alloy

As visible in Fig. 5, the simplest metallurgical states at high temperature among the three alloys are obtained for the Fe-based one. As for the two first alloys solidification should begin with the crystallization of pro-eutectic carbides. The TaC, as for the cobalt-based alloy, would start precipitating at very high temperature (about 2000°C), and grow alone over a broad temperature range (almost 500°C) before the appearance of the ferritic matrix. This develops over almost 100°C and solidification finishes near 1450°C with the eutectic part of solidification leading to a {BCC matrix + TaC} compound. During the cooling down to 1000°C, the microstructure stays double-phased (BCC Fe-based matrix + TaC).

Quantitatively (Fig. 6), a great mass fraction of pro-eutectic TaC (12-13 mass.%) already exists at the beginning of the eutectic reaction. This last reaction brings only about 5 mass.% of TaC. At 1200°C (Table 1), 16 mass.% (i.e. 9 vol.%) of TaC is present in the microstructure.

Microstructures of the alloys in the as-cast conditions

The manufacture of the three alloys from pure elements using the high frequency induction furnace (illustrated in Fig. 7) was seemingly successful, despite the high melting points of some of the elements (Cr, but also Fe, Co and Ni) and the obtained levitating liquid alloys seemed wholly molten for the maximum applied operating parameters (4 kV, 110kHz). A 3 minute stage at the maximum power was applied to ensure chemical homogenization of the molten alloys. The main parts of the alloys (centers of the ingots), the microstructures of which are illustrated in Fig. 8 and analyzed by XRD in Fig. 9, are described as:

- COhighTaC alloy: coarse, blocky TaC carbides (white facetted particles in BSE mode), dendritic matrix and script-like TaC carbides forming a eutectic with matrix in the interdendritic spaces;
- NIhighTaC alloy: blocky TaC carbides, dendritic matrix, interdendritic eutectic script-like tantalum carbides mixed with matrix and acicular chromium carbides forming a eutectic with matrix in some interdendritic spaces;
- FEhighTaC alloy: seemingly no blocky Ta (in contrast with the cobalt and nickel alloys), interdendritic eutectic {script-like TaC – matrix} and acicular eutectic {chromium carbide – matrix} compounds.

The XRD runs first showed that the tantalum carbides were really TaC (and not other types of tantalum carbides, such as Ta_2C), although that the corresponding peaks were very small by comparison to the matrix. When present (NIhighTaC and FEhighTaC alloys), the chromium carbides were not clearly detected by XRD, because of their fractions lower than the TaC ones. These are EDS spot analyses performed on the dark particles which allowed identifying them by indicating high concentrations in both chromium and carbon. The matrix was austenitic (FCC) for the NIhighTaC alloy and ferritic (BCC) for the FEhighTaC one, while the matrix of the

COhighTaC alloy was double-phased, FCC and HCP. The cooling was obviously too fast to allow the total transformation from austenite to the hexagonal phase.

The microstructures in the peripheries of the three ingots, illustrated in Fig. 10 (case of the NIhighTaC alloy), were quite different. There was obviously a local concentration of TaC blocky carbides, all around the ingot, and was worse for the FEhighTaC and NIhighTaC alloys than the cobalt alloy.

The chemical composition of the three as-cast alloys was specified by EDS analysis on central areas, globally and locally (matrix). The results (average and standard deviation from three global or spot measurements) are presented in Table 2 for the COhighTaC alloy, Table 3 for the NIhighTaC one and Table 4 for the FEhighTaC one.

It appears first that the tantalum content was lower than targeted, in the three alloys. This especially true for the NIhighTaC alloy (3 wt.%Ta less) and the COhighTaC one (9 wt.%Ta less). By considering that this decrease in Ta was certainly due to the observed migration to the ingot's periphery of a more or less high quantity of the TaC, the probable carbon content in the ingot's center (light element which cannot be specified by EDS) was calculated. The results are given in the last line of each table (the 1 for 1 atomic equivalence between Ta and C in the TaC carbides corresponds to about a 15 to 1 weight fraction equivalence). This leads to 0.9 wt.%C against 1 for the cobalt alloy (i.e. almost unchanged), 0.2 wt.% less than the targeted value for the nickel alloy and 0.6 wt.% less for the iron alloy, for which less than half of the total carbon content thus remains in the ingot's center. Similar to tantalum, the missing carbon atoms were at the peripheries of the ingots, as TaC carbides.

The Ta contents in the matrix depend on the alloy. It was the highest in the nickel alloy (Table 3) and the lowest in the iron one (Table 4). The Ta content in the COhighTaC matrix was intermediate (Table 3).

Discussion

Understanding of the obtained microstructures

The preliminary thermodynamic calculations run for successive levels of temperature allowed seeing that the start of solidification may occur by the crystallization of a carbide phase, and not with matrix, as the most often met for cast carbide-containing alloys. For the usual contents in carbon (and the corresponding tantalum to be atomically equal), for example 0.4 wt.% and 15 × 0.4 = 6 wt.% Ta, similar {25 to 30 wt.%Cr} – containing alloys based on Co[23], Ni[21] or Fe[16], solidification starts with the matrix (which grows with a dendritic shape) and finishes with the eutectic solidification of the residual interdendritic liquid as script-like TaC carbides mixed with matrix. Here, with 1 wt.%C and 15 wt.%Ta, there are two types of TaC carbides, with very characteristic morphologies. For alloys similar to those studied, but with more conventional carbon and tantalum contents, there are firstly script-like TaC carbides. They are mixed with matrix in the interdendritic spaces (resulting from the final part of solidification during which the residual liquid enriched in Ta and C due to chemical segregations was subjected to a eutectic {Liquid → Matrix + TaC} reaction). There were also other TaC carbides, coarser than the previous ones and blocky, present in the general microstructure and many of them concentrated along the periphery of the ingots. These are the TaC phase which appeared in the first instants of solidification, as revealed by the thermodynamic calculations. Their principal location (ingot's periphery) demonstrates that they effectively precipitated before the development of the dendritic network of matrix. Indeed this one did not obstruct the migration of the TaC toward the periphery. Such outward migration is similar to the one of no-molten parts or internal oxides of other alloys earlier elaborated in the laboratory with the HF induction furnace, migration promoted by the electromagnetic stirring inside the levitating molten alloy.

The most affected by the outward migration of the blocky pre-eutectic TaC carbides was the FEhighTaC alloy. This is because, firstly, the higher tendency to form many TaC with the available Ta, already observed[16], and here evidenced by the very low Ta content in matrix (Table 4). Secondly this was also favored by the very extended temperature range of its {Liquid; TaC} double-phased domain (Figs. 5 and 6).

Consequences of this phenomenon

Such migration of the pro-eutectic TaC carbides induces an impoverishment of the main part of the alloy. Its solidification can be modified consequently by the local change in chemical composition. Indeed, with this double impoverishment in C and Ta simultaneously (more for the FEhighTaC alloy than for the two other ones as evidenced by global EDS results) the center of ingot goes on solidifying as an alloy which contains less carbon and less tantalum. Except some rare pro-eutectic carbides remained in the center (maybe the last one to solidify and the more probably ones to be obstructed by the dendritic network of matrix), the rest of microstructure is quite similar to the ones of the {0.4-05wt.% C; 3 to 6 wt.%Ta}-containing Co-30Cr, Ni-30Cr or Fe-30Cr alloys earlier studied[16,21,23].

The microstructural development is destabilized anyway. Indeed it is difficult to describe the solidification progress of a so open system (with TaC quitting the solidifying alloy), and the process may be influenced by parameters as cooling rate in additional fields to the only microstructure fineness. This outward TaC migration, which is here favored by the particular electromagnetic stirring in laboratory conditions, may probably exist also, maybe in a lower magnitude, in melting of several kilograms in a more industrial context. Indeed the difference of volume mass of pre-eutectic TaC and still liquid alloy may induce slow but existing gravitational down moving of TaC toward the ingot bottom, but in such conditions the development of the dendritic network capable to obstructing this TaC movement should also be slow, because of low cooling rate.

Efficiency of the used database; new calculations to carry out

Thus the chemical compositions may be efficiently modified and rated in order to obtain more TaC carbides, only of a eutectic nature. Such work can be done by modifying the C and Ta contents, but why not the Cr content too? For example, the phase diagrams presented in Fig. 1 (cobalt alloys) and Fig. 5 (iron alloys) suggest respectively that a decrease in chromium from the COhighTaC alloy may decrease a little the temperature range of the {Liquid + TaC} domain and an increase in Cr ought to have the same effect but more marked for the FEhighTaC alloy.

However, the database used is not very accurate for the cobalt alloys, as proven by the existence of TaC only as carbide phase in the really obtained microstructure, although small quantities of chromium carbides were expected. This is true for the iron alloys since chromium carbides are significantly present with typical solidification morphologies in contradiction with the thermodynamic calculations. In the first case, this is possibly the rather high cooling rate which did not allow carbide transformations as soon as the temperature is low enough (typically 300°C under solidification) and only limited transformation of the matrix (remained two-phase FCC + HCP, while calculations for low temperatures lead to only HCP). This is the reason why the predictions for medium and low temperatures were not presented in the phase diagrams. In the case of the FEhighTaC, alloy this is the presence of chromium carbides in the obtained alloy which is surprising. This can be explained by the chemical, then thermodynamic destabilization of the alloy during its solidification by the massive loss of TaC migrating toward the ingot's periphery. Indeed, tantalum and carbon atoms were took away by this outward TaC migration. This changed the local chemical composition and thermodynamic equilibria, perturbing the following of solidification and favoring the appearance of chromium carbides.

The database used was already exploited in earlier studies concerning cobalt-base[23] and iron-based[16] alloys with lower contents in Ta and C, with good agreement between thermodynamic calculations and obtained as-cast microstructures as well as isothermally aged ones. Thermodynamic calculations and real microstructures matched less well for the nickel-based alloy. Tantalum carbides were not predicted by calculations, with carbon only involved in chromium carbides and tantalum dissolved in the developing matrix during solidification, and both in the matrix and in an intermetallic compound after solidification. The alloy obtained was quite different, since chromium carbides were effectively present in rather great quantities but eutectic TaC (and also pro-eutectic TaC) were significantly present in the as-cast microstructure of the NIhighTaC alloy. The same mismatch was found earlier, for similar nickel-chromium alloys containing less carbon and less tantalum[21], between calculations carried out with the same software and the same database. But this was essentially due to the fast solidification of the experimental alloys. Indeed, all the

tantalum carbides disappeared during only 50 hours isothermal treatment at high temperatures.

Conclusions

The tantalum carbides are known in the cast superalloy's world to be particularly efficient in high temperature strengthening. This is due to their interdendritic location, script morphology, high refractoriness and good stability in hot conditions. Here these TaC carbides were obtained with particularly great fractions in these alloys highly alloyed with carbon and tantalum. Unfortunately, the increase in C and Ta from the usual values, led to TaC carbides of two types: script eutectic ones mixed with matrix as for lower C and Ta contents, and also coarse blocky ones. These ones are probably less favorable to good mechanical resistance at high temperature. Thermodynamic calculations allowed understanding when the TaC carbides of this new type precipitated during solidification, and furthermore why they tended to migrate from the ingot's center by going to the periphery (Fig. 10). Future experimental work must be done, characterizing the consequences of these particular microstructures for the mechanical properties at high temperature. At the same time, future thermodynamic calculations will aim to select intermediate C and Ta contents allowing the avoidance of the pro-eutectic carbides which causes an overconsumption of the expensive Ta element and which possibly compromises the mechanical properties. This possible weakening will be later studied, for example, by creep tests and comparison with alloys slightly impoverished in C and Ta but free of pre-eutectic TaC.

One can point out that the experimental part of this work was carried out with rather small ingots (masses of only 40g, size of a few centimeters. Although they preliminarily allowed obtaining or observing interesting results and unexpected phenomena, permitting to anticipate possible analogous phenomena and their consequences for much greater dimensions of castings, the case of alloys cast at higher scales is to be further investigated.

To finish one can remind the potential strengthening of so high fractions of TaC carbides for superalloys classically cast to allow complex geometries of hot pieces. With so high degree of imbrication of matrix and script-like refractory and stable carbides one can guess that the service temperature under mechanical stress may increase to come close to the melting start temperature of the alloys, as is to say 1200°C and probably slightly higher. This is much more than what is possible for the currently best superalloys, the γ/γ' nickel-based single-crystals since, at such temperature which is higher than the γ'-solvus temperature, their reinforcing precipitates ought have totally disappear with consequently total loss of their strength. Thus, even tantalum is a very expensive element, the cost induced by so high contents in Ta probably remain competitive with the high cost of fabrication of single crystals. If further characterization will confirm the mechanical interest of highly TaC-strengthened alloys for pieces playing a key role at elevated temperature the cost of tantalum will be rapidly forgotten.

Acknowledgements:

The authors thank Thierry Schweitzer who helped them in the cutting of these rather hard alloys for providing the necessary parts for metallographic characterization.

References:

1. X. Zhang, X. Bai, X. Cai, Y. Zhang, F. Wang, and H. Wang: 'Surface strengthening of Ta-C compound cladded for tantalum alloy', *Xiyou Jinshu Cailiao Yu Gongcheng*, 2012, **41(10)**, 1761-1764.

2. P. Bala: 'Microstructure characterization of high carbon alloy from the Ni-Ta-Al-Co-Cr system', *Archives of Metallurgy and Materials*, 2012, **57(4)**, 937-941.

3. M. Y. Li, M. J. Chao, E. J. Lang, D. C. Li, J. M. Liu, and J. J. Zhang: 'Laser synthesized TaC for improving copper tribological property', *Surface Engineering*, 2013, **29 (8)**, 616-619.

4. C. Balagna, M. G. Faga, and S. Spriano: ‘Tribological behaviour of a Ta-based coating on a Co-Cr-Mo alloy’, *Surface and Coatings Technology*, 2014, Ahead of Print.

5. H. Tanaka, S. Mouri, K. Nakahara, H. Sano, G. B. Zheng, B. Guo, and Y. Uchiyama: ‘Oxidation behaviour of sintered WC-TiC-TaC alloys’, *Nippon Tungsten Review*, 2007, **39**, 1-8.

6. M. Naidoo, O. Johnson, I. Sigalas, and M. Herrrmann; ‘Preparation of Ti-Ta-(C,N) by mechanical alloying Ti(C,N) and TaC’, *International Journal of Refractory Metals & Hard Materials*, 2013, **37**, 67-72.

7. D. Xia, K. Chan, and S. Wang; ‘Microstructure and properties of WC-(W,Ti)C-(Ta,Nb)C-Co coated carbide alloy’, *Jinshu Rechuli*, 2009, **34(1)**, 19-22.

8. E. M. Salley, and Z. Hussain; ‘Characterization of tantalum carbide reinforced copper composite developed using mechanical alloying’, *Key Engineering Materials*, 2011, **471-472**, 798-803.

9. I. Narita, S. Sakamoto, H. Miyahara, K. Yamamoto, K. Kamimyada, and K. Ogi; ‘Solidification microstructures and quench/temper hardness of tantalum added high-carbon high-speed steel type cast alloy’, *Materials Transactions*, 2012, **53(2)**, 354-361.

10. K. Nakama, K. Sugita, and Y. Shirai; ‘Effect of MC type carbides on age hardness and thermal expansion of Fe-36 wt%Ni-0.2 wt%C alloy’, *Metallography and Analysis*, 2013, **2(6)**, 383-387.

11. S. H. Chang, J. R. Huang, C. C. Lin, and C. Liang; ‘Effects of vacuum sintering process on the microstructure and strengthening mechanisms of tantalum carbides added Ti-Cu-Mo alloys’, *Kuangye*, 2013, **57(4)**, 78-83.

12. T. Depka, Ch. Somsen, G. Eggeler, D. Mukherji, J. Roesler, M. Krüger, H. Saage, and M. Heilmaier; ‘Microstructures of Co-Re-Cr, Mo-Si and Mo-Si-B high-temperature alloys’, *Materials Science & Engineering A: Structural Materials: Properties, Microstructure and Processing*, 2009, **A510-A511**, 337-341.

13. T. Zhao, J. Zhang, G. Chen, and L. Lou; 'Effect of Re and Ta addition ion the formation and decomposition of primary carbides in a 2nd generation DS superalloy', *Xiyou Jinshu Cailiao Yu Gongcheng*, 2009, **38(6)**, 1038-1042.

14. A. Schneider, L. Falat, G. Sauthoff, and G. Frommeyer; 'Constitution and microstructures of Fe-Al-M-C (M=Ti, V, Nb, Ta) alloys with carbides and Laves phase', *Intermetallics*, 2003, **11(5),** 443-450.

15. L. Falat, A. Schneider, G. Sauthoff, and G. Frommeyer; 'Mechanical properties of Fe-Al-M-C (M=Ti, V, Nb, Ta) alloys with strengthening carbides and Laves phase', *Intermetallics*, 2005, **13(12)**, 1256-1262.

16. P. Berthod, Y. Hamini, L. Aranda, and L. Héricher; 'Experimental and thermodynamic study of tantalum-containing iron-based alloys reinforced by carbides: Part I-Case of (Fe, Cr)-based ferritic steels', *Calphad*, 2007, **31(3)**, 351-360.

17. P. Berthod, Y. Hamini, L. Héricher, and L. Aranda; 'Experimental and thermodynamic study of tantalum-containing iron-based alloys reinforced by carbides: Part II-Case of (Fe, Ni, Cr)-base austenitic steels', *Calphad*, 2007, **31(3)**, 361-369.

18. U. Brill; 'Carbide strengthening of wrought nickel-base alloys', *Advanced Engineering Materials*, 2001, **3(11)**, 916-921.

19. L. Zheng, C. Gu, and G. Zhang; 'Effect of Ta addition on microstructure of cast nickel base superalloys containing low level of Cr and high level of W', *Xiyou Jinshu Cailiao Yu Changcheng*, 2005, **34(2)**, 194-198.

20. A. Janas, A. Kolbus, and E. Olejnk; 'Carbide strengthening of wrought nickel-base alloys', *Advanced Engineering Materials*, 2001, **3(11)**, 916-921.

21. P. Berthod, L. Aranda, C. Vébert, and S. Michon; 'Experimental and Thermodynamic Study of the Microstructural State at High Temperature of Nickel base Alloys containing Tantalum', *Calphad*, 2004, **28(2)**,159-166.

22. S. Michon, P. Berthod, L. Aranda, C. Rapin, R. Podor, and P. Steinmetz; ‘Application of thermodynamic calculations to study high temperature behavior of TaC-strengthened Co-base superalloys’, *Calphad*, 2003, **27(3)**, 289-294.

23. P. Berthod, S. Michon, L. Aranda, S. Mathieu, and J.C. Gachon; ‘Experimental and thermodynamic study of the microstructure evolution in cobalt-base superalloys at high temperature’, *Calphad*, 2003, **27(4)**, 353-359.

24. Z. Opiekun, and K. Chrusciel; ‘Structural studies of partial meltings of casting surfaces made of cobalt alloy MAR-M509’, *Archives of Foundry Engineering*, 2009, **9(2)**, 197-200.

25. Thermo-Calc version N: "Foundation for Computational Thermodynamics" Stockholm, Sweden, Copyright (1993, 2000). www.thermocalc.com

26. SSOL database, SGTE (Scientific Group Thermodata Europe), update 1992.

27. K. Frisk, and A. Fernandez Guillermet; ‘Gibbs energy coupling of the phase diagram and thermochemistry’, *Journal of Alloys and Compounds*, 1996, **238**, 167-179.

28. Z.K. Liu, and Y. Austin Chang; ‘Thermodynamic assessment of the Co-Ta system’, *Calphad*, 1999, **23**, 339-356.

29. N. Dupin, and I. Ansara; ‘Thermodynamic assessment of the Cr-Ta system’, *Journal of Phase Equilibria*, 1993, **14**, 451-456.

30. L. Dimitrescu, M. Ekroth, B. Jansson; ‘Thermodynamic assessment of the Me-Co-C systems (Me=Ti, Ta or Nb)’, *Metallurgical Transactions A* , 2001, **32A**, 2167-2174.

31. Handbook of Chemistry and Physics, 57th edition, 1976-1977.

Table 1. Theoretical fractions of carbides at 1200°C according to Thermo-Calc for the Co (bal.)-30Cr-1C-15Ta, Ni (bal.)-30Cr-1C-15Ta and Fe (bal.)-30Cr-1C-15Ta (wt.%) compositions

Carbides fractions	TaC		Cr_xC_y	
	mass.%	vol.%*	mass.%	vol.%
COhighTaC	13.89	8.72*	/	/
NIhighTaC	5.56	4.02**	16.86	20.56**
FEhighTaC	15.83	9.21***	/	/

Calculations performed using:
- the average value of the Ni_3Ta densities given by [27, 28] (11.38g/cm^3 and 12.04 g/cm^3) [31], 14.5 g/cm^3 for the TaC's one, and 6.946 g/cm^3 for the average Cr_xC_y's one (6.941 for Cr_7C_3 and 6.953 $Cr_{23}C_6$) [31]
- and using 8.9 g/cm^3 (* and **) and 7.6 g/cm^3 (***) for the matrix density.

Table 2. Chemical compositions of the ingots' core for the as-cast COhighTaC alloy: global composition (3 areas ×1000) and matrix composition (3 spots), SEM-EDS analysis

COhighTaC	global		matrix	
	average	std dev	average	std dev
Cr (wt.%)	31.4	0.8	33.0	2.2
Ta (wt.%)	13.7	1.4	3.3	0.3
Supposed local C content (= 1-ΔTa/15)	0.91 (against 1 wt.%)			

ΔTa= targeted Ta content – Ta content measured (EDS) in ingot's core (wt.%)

Table 3. Chemical compositions of the ingots' core for the as-cast NIhighTaC alloy: global composition (3 areas ×1000) and matrix composition (3 spots), SEM-EDS analysis

NIhighTaC	global		matrix	
	average	std dev	average	std dev
Cr	31.8	0.8	30.0	0.9
Ta	12.0	1.4	6.0	0.4
Supposed local C content (= 1-ΔTa/15)	0.80 (against 1 wt.%)			

ΔTa= targeted Ta content – Ta content measured (EDS) in ingot's core (wt.%)

Table 4. Chemical compositions of the ingots' core for the as-cast FEhighTaC alloy: global composition (3 areas ×1000) and matrix composition (3 spots), SEM-EDS analysis

FEhighTaC	global		matrix	
	average	std dev	average	std dev
Cr	35.6	2.1	33.5	0.6
Ta	5.8	1.3	0.5	0.1
Supposed local C content (= 1-ΔTa/15)	0.39 (against 1 wt.%)			

ΔTa= targeted Ta content – Ta content measured (EDS) in ingot's core (wt.%)

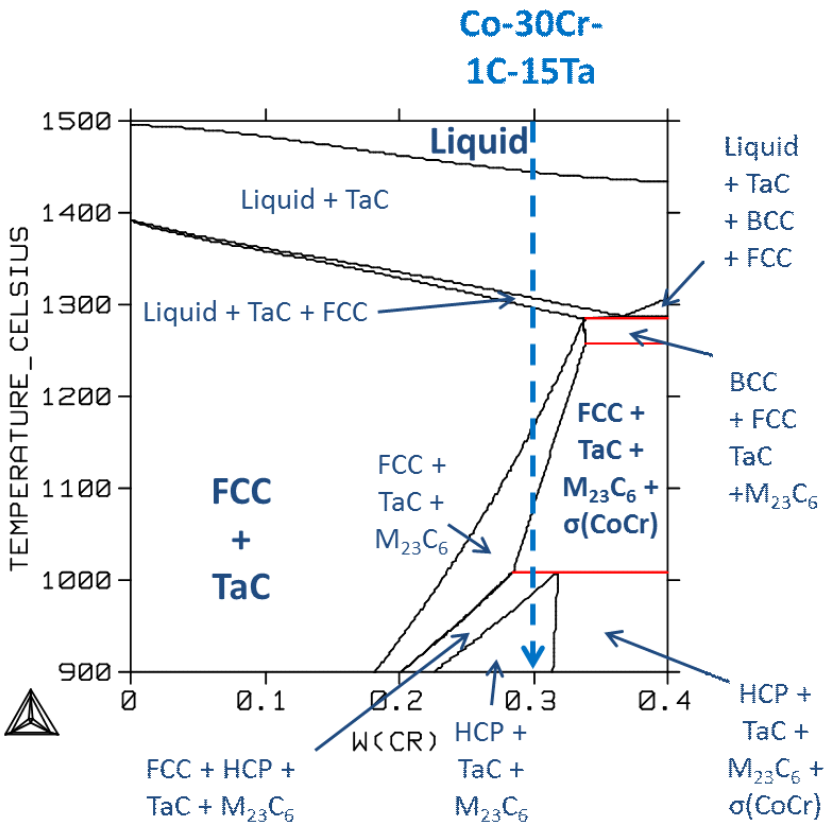

Fig. 1. Phase diagram visualizing qualitatively the theoretical solidification of the “COhighTaC” alloy (Thermo-Calc)

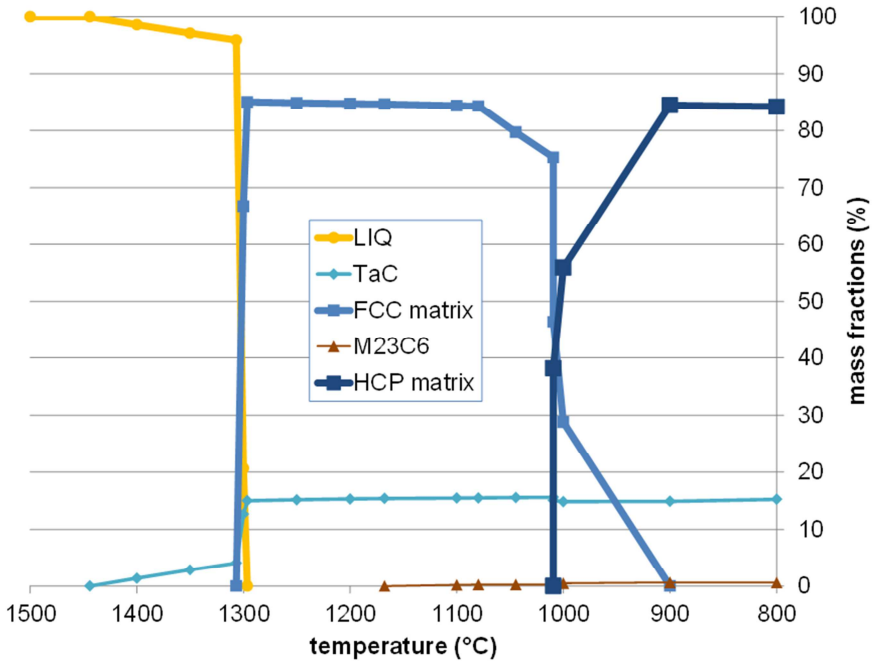

Fig. 2. Preliminary thermodynamic calculations describing quantitatively the theoretical solidification of the “COhighTaC” alloy (Thermo-Calc)

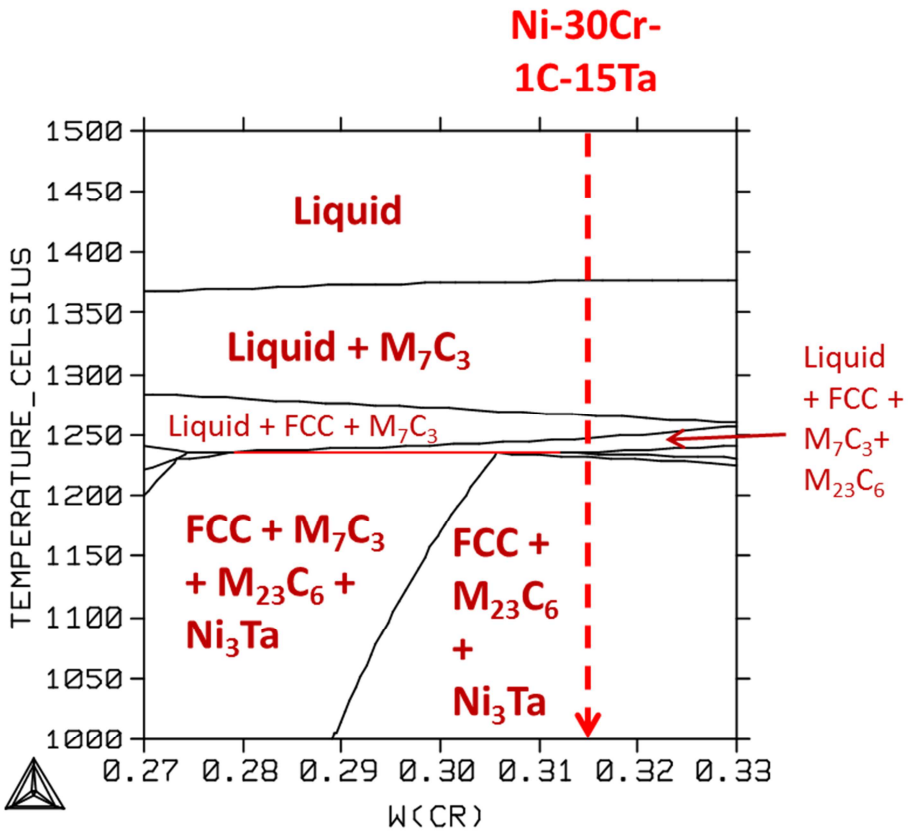

Fig. 3. Phase diagram visualizing qualitatively the theoretical solidification of the “NIhighTaC” alloy (Thermo-Calc)

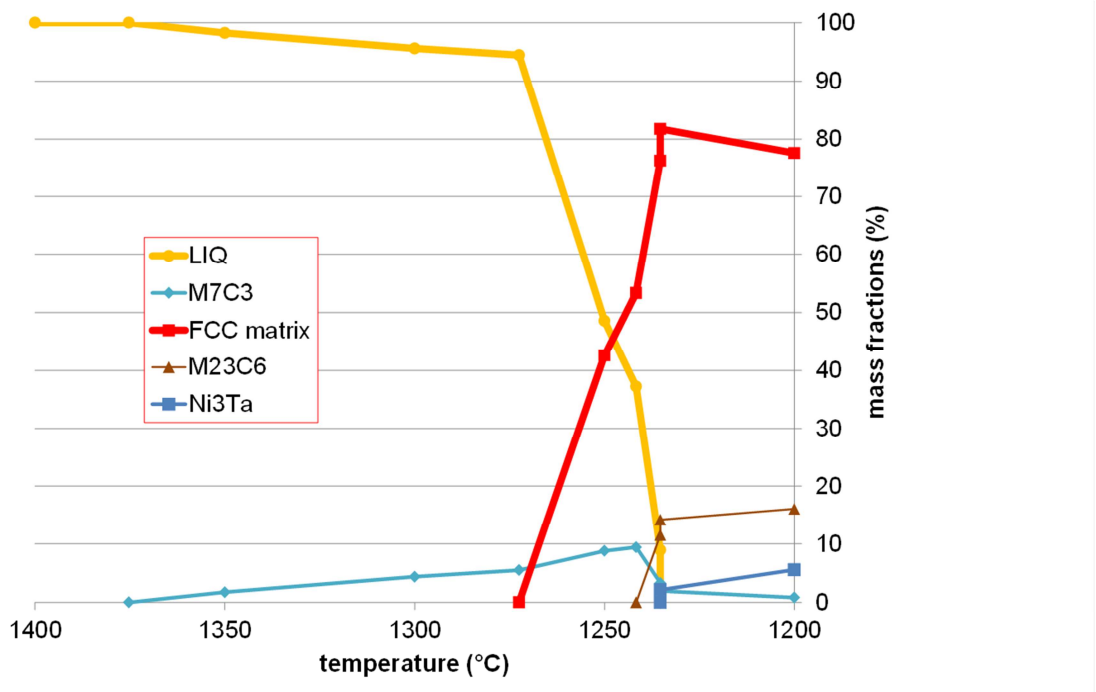

Fig. 4. Preliminary thermodynamic calculations describing quantitatively the theoretical solidification of the “NIhighTaC” alloy (Thermo-Calc)

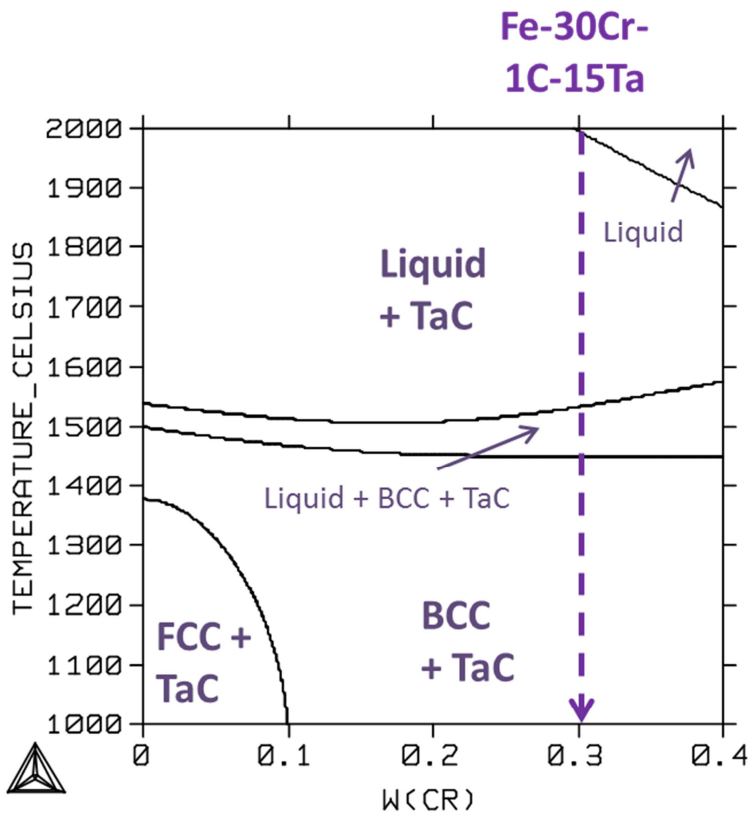

Fig. 5. Phase diagram visualizing qualitatively the theoretical solidification of the “FEhighTaC” alloy (Thermo-Calc)

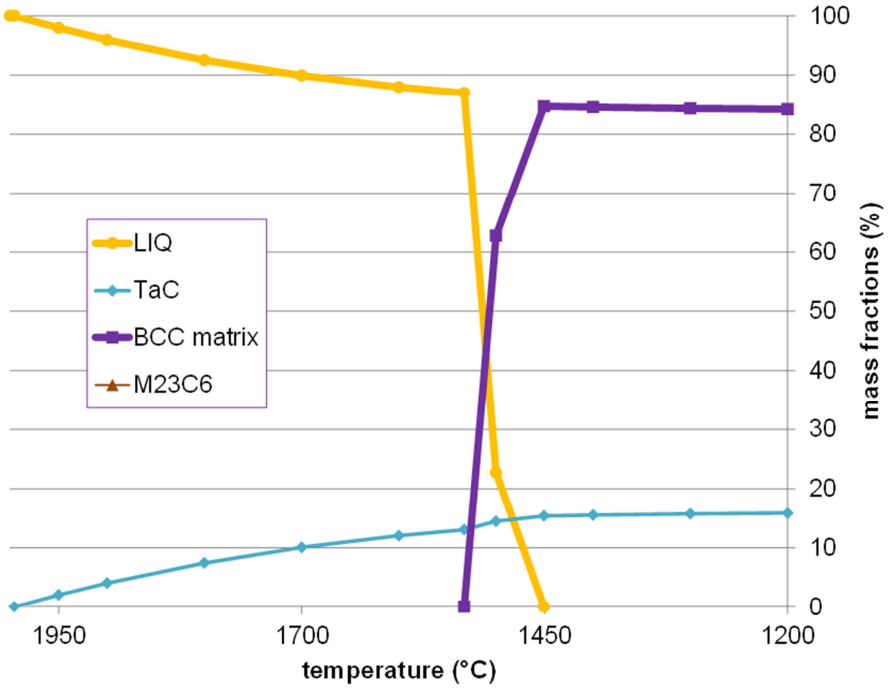

Fig. 6. Preliminary thermodynamic calculations describing quantitatively the theoretical solidification of the “FEhighTaC” alloy (Thermo-Calc)

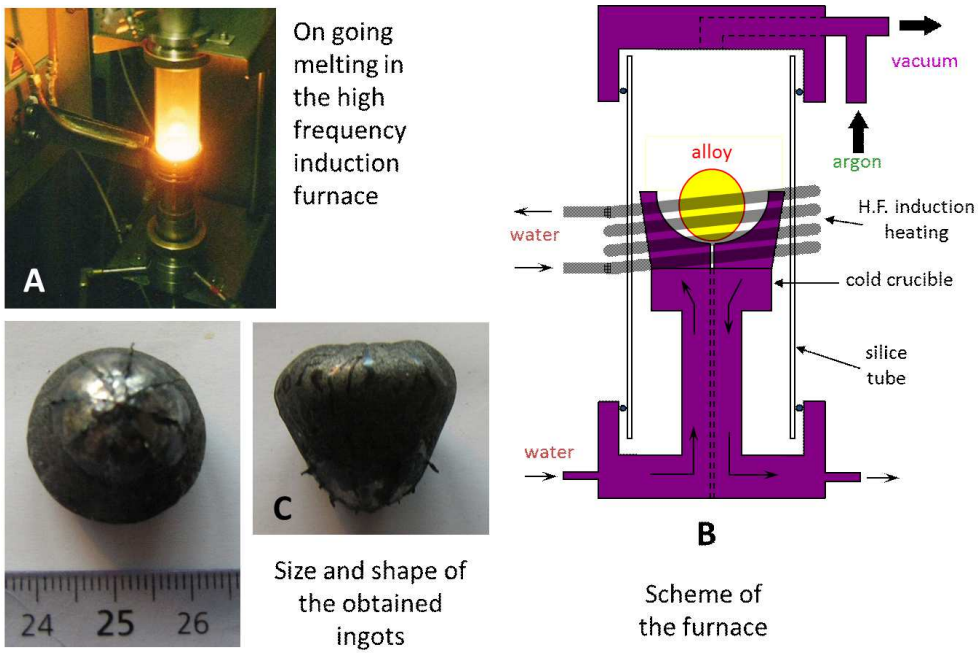

Fig. 7. Photograph of the melting chamber of the High Frequency induction furnace during the elaboration of one of the alloys (A); scheme describing this hottest part of the apparatus (B); photographs of an ingot (C)

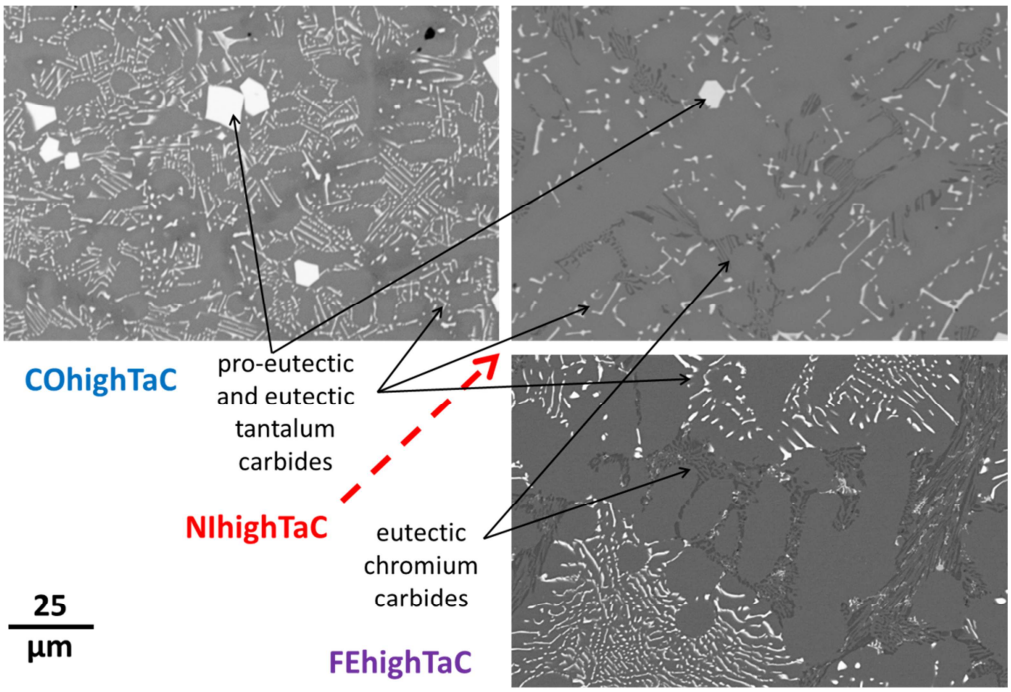

Fig. 8. Microstructures the three alloys in their as-cast states (SEM/BSE micrographs)

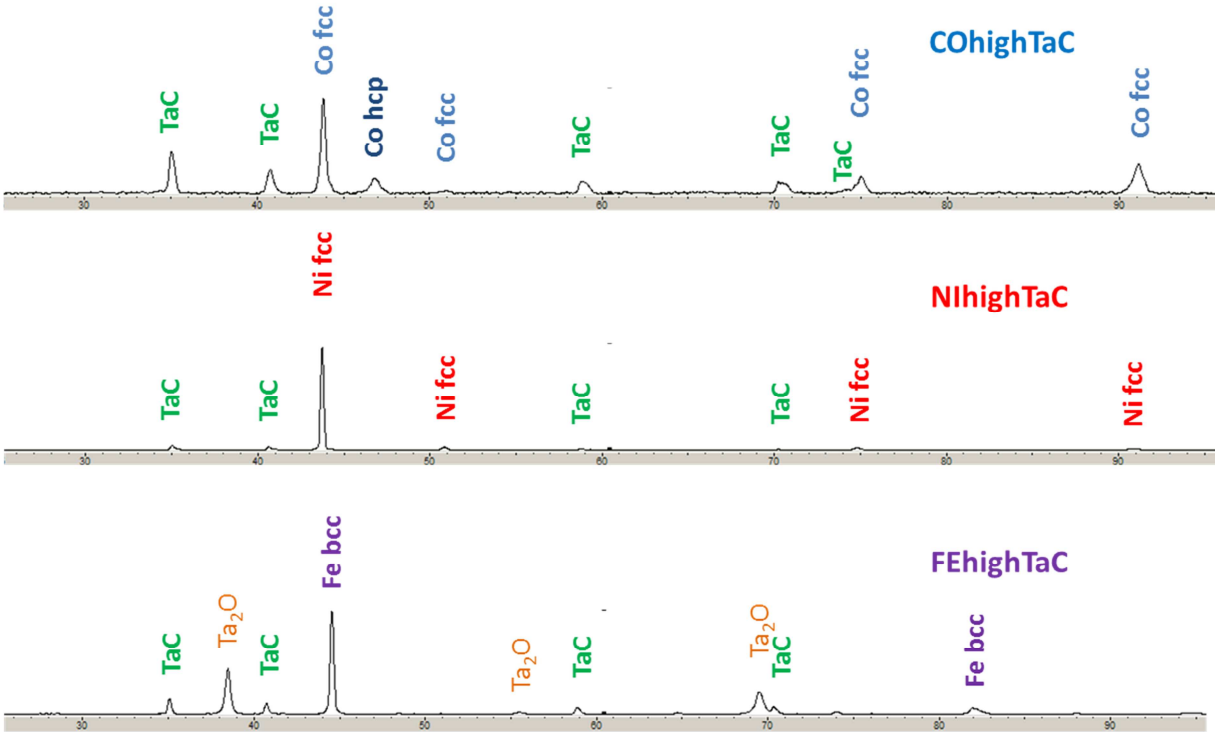

Fig. 9. XRD diffractograms acquired on the three as-cast alloys (top: the cobalt-based alloy, middle: the nickel-based alloy, bottom: the iron-based alloy)

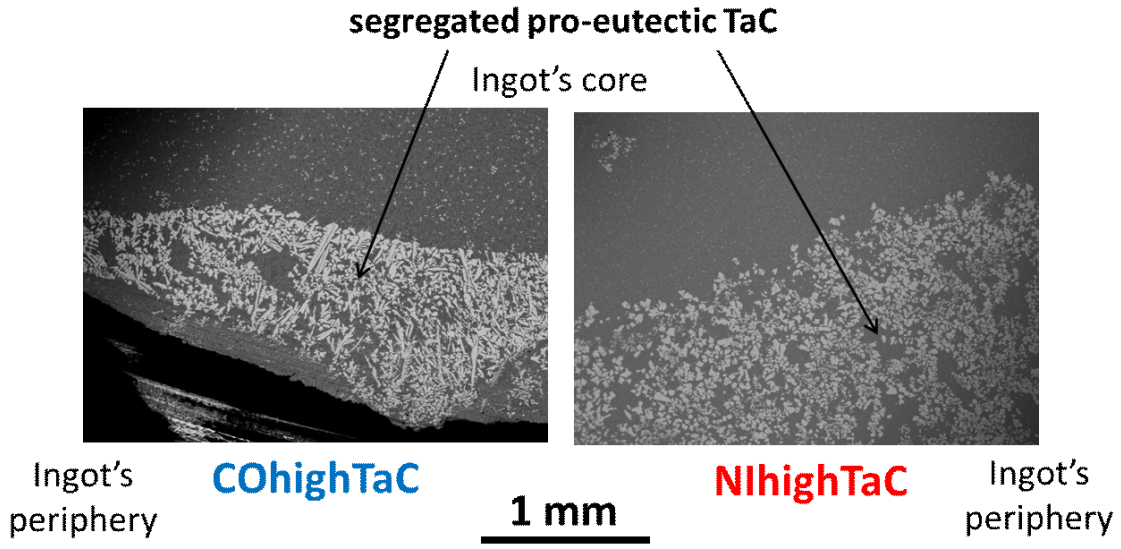

Fig. 10. Illustrations of the outward segregation of TaC carbides as evidenced in the periphery of the ingot (SEM/BSE micrographs)